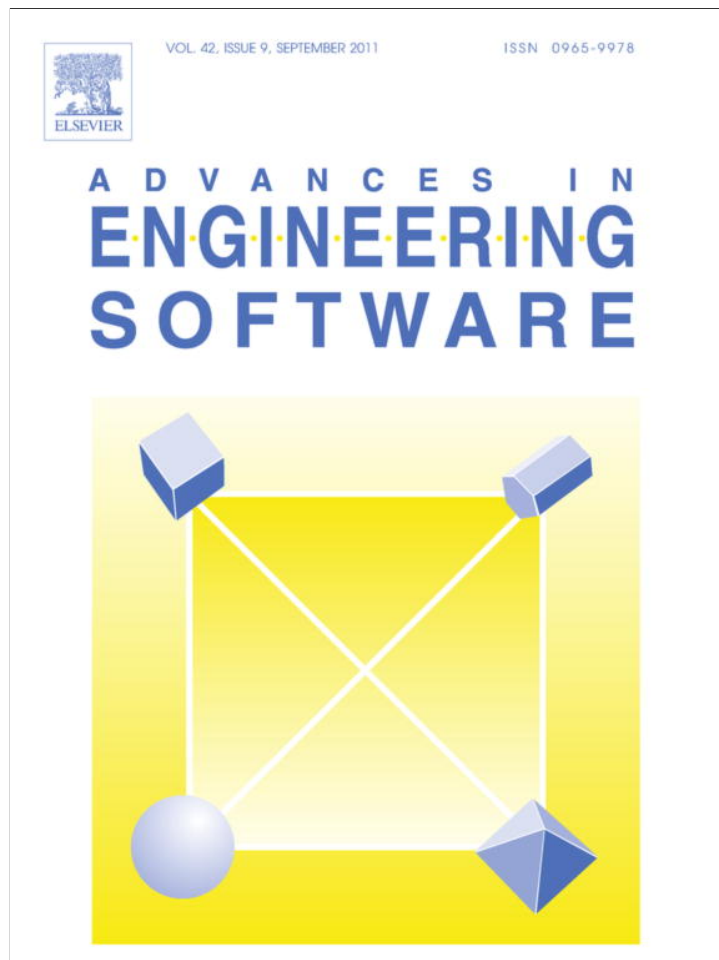


Provided for non-commercial research and education use.  
Not for reproduction, distribution or commercial use.



This article appeared in a journal published by Elsevier. The attached copy is furnished to the author for internal non-commercial research and education use, including for instruction at the authors institution and sharing with colleagues.

Other uses, including reproduction and distribution, or selling or licensing copies, or posting to personal, institutional or third party websites are prohibited.

In most cases authors are permitted to post their version of the article (e.g. in Word or Tex form) to their personal website or institutional repository. Authors requiring further information regarding Elsevier's archiving and manuscript policies are encouraged to visit:

<http://www.elsevier.com/copyright>



Contents lists available at ScienceDirect

## Advances in Engineering Software

journal homepage: [www.elsevier.com/locate/advengsoft](http://www.elsevier.com/locate/advengsoft)

## 1D unified mathematical model for environmental flow applied to steady aerated mixed flows

F. Kerger<sup>a,b,\*</sup>, S. Erpicum<sup>a</sup>, B.J. Dewals<sup>a,b</sup>, P. Archambeau<sup>a</sup>, M. Piroton<sup>b</sup>

<sup>a</sup>Research Unit of Hydrology, Applied Hydrodynamics and Hydraulic Constructions (HACH), ArGenCo Department, University of Liège, 1 allée chevreuils, 4000 Liège, Belgium  
<sup>b</sup>Belgian Fund for Scientific Research, F.R.S-FNRS, Belgium

## ARTICLE INFO

## Article history:

Received 18 September 2009  
 Received in revised form 27 April 2011  
 Accepted 28 April 2011  
 Available online 28 May 2011

## Keywords:

Finite volume method  
 Homogeneous Equilibrium Model  
 Preissmann slot  
 Local Instant Formulation  
 Air-entrainment  
 Civil engineering  
 Hydraulic engineering

## ABSTRACT

Hydraulic models available in literature are unsuccessful in simulating accurately and efficiently *environmental flows* characterized by the presence of both air–water interactions and free-surface/pressurized transitions (aka mixed flows). The *purpose* of this paper is thus to fill this knowledge gap by developing a unified one-dimensional mathematical model describing free-surface, pressurized and mixed flows with air–water interactions. This work is part of a general research project which aims at establishing a unified mathematical model suitable to describe the vast majority of flows likely to appear in civil and environmental engineering (pure water flows, sediment transport, pollutant transport, aerated flows...). In order to tackle this problem, our original *methodology* consists in both time- and space-averaging the Local Instant Formulation, which includes field equations for each phase taken separately and jump conditions, over a flow cross-section involving a free-surface. Subsequently, applicability of the model is extended to pressurized flows as well. The first key *result* is an original 1D Homogeneous Equilibrium Model which describes two-phase free-surface flows. It is proven to be fundamentally multi-phase, to take into account scale heterogeneities of environmental flow and to be very easy to solve. Next, applicability of this free-surface model is extended to pressurized flows by using the classical Preissmann slot concept. A second key result here is the introduction of an original negative Preissmann slot to simulate sub-atmospheric pressurized flows. The model is then closed by using constitutive equations suitable for air–water flows. Finally, this mathematical model is discretised by means of a finite volume scheme and validated by comparison with experimental results from a physical model in the case of a steady flow in a large scale gallery.

© 2011 Elsevier Ltd. All rights reserved.

## 1. Introduction

Civil and environmental engineers make frequent use of mathematical and numerical models to handle with hydraulics problems. In this respect, the need for consistent mathematical and numerical models has never been more pressing. The acuteness of the situation is prompted by growing concerns about ecological, technical and economic issues. As an evocative example of such a hydraulic problem, one can cite mixed flows, characterized by the simultaneous occurrence of free-surface and pressurized flows (Fig. 1). This flow pattern is frequently encountered in rivers networks (water intakes and deviations in closed pipes), sewer systems, storm-water storage pipes, flushing galleries, bottom outlets, ... As a matter of fact, some hydraulic structures are designed to combine free-surface and pressurized sections (e.g. water

intakes). In addition, dynamic pipe filling bores may occur in hydraulic structures designed only for conveying free-surface flow under an extreme water inflow or upon starting a pump [1,2]. During such a transition, highly transient phenomena appear and may cause structural damages to the system [3], generate geysers through vertical shafts [4], engender flooding, ... What is more, air/water interactions may arise, particularly at the transition bore [5], and alter thoroughly the flow regime and its characteristics. On account of the range of applications affected by mixed flows, a good prediction of its features is an industrial necessity.

Scientific literature offers different mathematical approaches to describe mixed flows. First, the so-called *shock-tracking approach* consists in solving separately free-surface and pressurized flows through different sets of equations [6,7]. The advantage of this method is that the transition is computed as a true discontinuity (infinite resolution). Such an algorithm is very complicated and case-specific so that it is difficult to apply it to practical applications. Important experimental information on the transition motion is given by Cardle and Song [6]. As a particular case of shock-tracking approach, the Rigid Water Column Approach [7]

\* Corresponding author at: Research Unit of Hydrology, Applied Hydrodynamics and Hydraulic Constructions (HACH), ArGenCo Department, University of Liège, 1 allée chevreuils, 4000 Liège, Belgium. Tel.: +32 43 66 90 04.

E-mail address: [fkерger@ulg.ac.be](mailto:fkерger@ulg.ac.be) (F. Kerger).



**Fig. 1.** Mixed flow typical configuration involves an air–water pressurized flow and a free-surface flow separated by a moving transition.

treats each phase (air/water) separately on the basis of a specific set of equations. The latter approach succeeds in simulating complex configurations of the transition but fails in its attempt to describe all flow regimes. Using the method for practical application is also difficult because of the complexity and specificity of the algorithm. Second, the so-called *shock-capturing* approach is a family of method which computes pressurized and free-surface flows by using a single set of equations [8–11]. The most widespread of these methods is the Preissmann slot [8,12] because it only uses the classical Saint–Venant equations [13]. Such a model is however unable to simulate sub-atmospheric pressurized flows [14]. Recently, research focuses to integrate the effect of the air phase on the behavior of mixed flows. To authors' knowledge, two methods integrate the effect of pressurization of the air phase above the free-surface: the Rigid Water Column [7] and the shock-capturing model of Vasconcelos [9,15]. However, these models do not account for the dispersed air in the water flow (air bubbles and pockets).

On account of this literature review, one can say that present models fail to simulate the presence of dispersed air in the water and free-surface/pressurized flow in a unified framework. The purpose of this paper is thus to fill this knowledge gap by developing a unified one dimensional mathematical model describing free-surface, pressurized and mixed flows with air entrainment. This work is part of a general research project which aims at establishing a unified mathematical model suitable to describe the vast majority of flows likely to appear in civil and environmental engineering. It includes pure-water flows, sediment transport over a mobile bed, pollutant transport, aerated flows... Four conditions are sought in the development of the model:

- The model must take into account accurately the motion of a dispersed air phase in water flow, and in particular it should describe efficiently the interaction of the water flow with the dispersed phase and the external environment.
- The model must handle correctly the scale heterogeneities in time and space, which are characteristic of practical applications and mechanisms encountered in free-surface and pressurized hydraulics.
- The model must treat in a unified framework mixed flows, characterized by the simultaneous occurrence of free-surface and pressurized flows.
- The model must require a moderate computational effort to solve most of practical cases in civil and environmental engineering (such that 3D models are not considered here).

Therefore, this paper proposes an original 1D Homogeneous Equilibrium Model (HE-Model) for free-surface flows whose applicability is extended to pressurized and mixed flows by means of the classical Preissmann slot and an original negative Preissmann slot. This model is proven to meet the previous objectives in many respects. The paper is divided in two parts. The first one exposes the derivation of the original mathematical model and the numerical scheme used to solve it. In the second part, we present the application of this new model to the case of flows in a gallery. Experimental results from a physical model build in the Laboratory of Engineering Hydraulics of the University of Liege are used for comparison with numerical results.

## 2. Unified mathematical model

### 2.1. Three-dimensional homogeneous flow model

If we assume that each sub-region bounded by interfaces in an air–water flow may be considered as a continuum, the standard single-phase Navier–Stokes equations holds for each sub-region with appropriate jump and boundary conditions. This is the Local Instant Formulation (LIF) which is extensively derived and commented in [16,17]. In principle, a two-phase flow model should solve the Local Instant Formulation. Obtaining a solution this way is however mathematically difficult and beyond the present computational capability for many engineering applications. On account of this, practical model have been developed. Most of them are derived by application of an averaging procedure on the LIF. In the present work, the Eulerian time averaging procedure is chosen because it is proven to be particularly useful for turbulent two-phase flow. Mathematical operation lead to the drift-flux model [18]. In this method, it is assumed that the multiphase flow may be described as a single phase flow of mixture variables that refer to the motion of the center of mass. The motion of the dispersed phase is then treated in terms of diffusion through the mixture. Since the momentum equation for this phase is neglected, a constitutive equation for the relative velocity is required.

In particular, the drift-flux model simplifies into the Homogeneous Equilibrium Model (HE-Model) if all phases are assumed to move at the same velocity (the relative velocity is negligible). The model is commonly used for the simulation of heat exchangers [19,20], two-phase flow in ducts [21],... For further details, we refer the interested reader to the classical book of Ishii and Hibiki [16]. The resulting field equations contain a continuity equation, a diffusion equation and a momentum equation:

$$\begin{cases} \frac{\partial \rho_m}{\partial t} + \nabla \cdot (\rho_m \mathbf{v}_m) = 0 \\ \frac{\partial \alpha_g}{\partial t} + \nabla \cdot (\alpha_g \mathbf{v}_m) = \Gamma_g \\ \frac{\partial \rho_m \mathbf{v}_m}{\partial t} + \nabla \cdot (\rho_m \mathbf{v}_m \mathbf{v}_m) = -\nabla p_m + \nabla \cdot (\tau_m + \tau^T) + \rho_m \mathbf{g} + \mathbf{M}_m \end{cases} \quad (1)$$

where  $\rho_m$  [kg/m<sup>3</sup>] is the mixture density,  $\mathbf{v}_m$  [ms<sup>-1</sup>] is the mixture velocity vector (under the assumption of velocity equilibrium,  $\mathbf{v}_m = \mathbf{v}_{\text{water}} = \mathbf{v}_{\text{air}}$ ),  $\alpha_g$  [-] is the air void fraction,  $\Gamma_g$  [s<sup>-1</sup>] is the phase change volume generation,  $p_m$  [Nm<sup>-2</sup>] is the mixture pressure,  $\tau_m$  [Nm<sup>-2</sup>] and  $\tau^T$  [Nm<sup>-2</sup>] are the viscous and turbulent stress tensors,  $\mathbf{g}$  [ms<sup>-2</sup>] is the gravity and  $\mathbf{M}_m$  [kg s<sup>-2</sup> m<sup>-2</sup>] is the interfacial momentum source. It is worthwhile noting that the simplicity of Eq. (1) results from the wise choice of the mixture macroscopic properties (i.e. mixture center of mass velocity, mixture density, mixture pressure...).

Closure of the HE-model requires the definition of the mixture variables and a constitutive equation. Air and water are supposed to be incompressible Newtonian fluids. The assumption of incompressibility may seem inappropriate, especially for pressurized flows. Hopefully, the compressibility of both fluids is accounted for a posteriori when extending applicability of the free-surface model to pressurized flows (see Section 2.4). The value of the celerity takes indeed into account the compressibility of the fluid. Consequently, the mixture properties are written as:

$$\begin{aligned} \rho_m &= \alpha_g \rho_g + (1 - \alpha_g) \rho_w \cong (1 - \alpha_g) \rho_w \\ \tau_m &= [\alpha_g \mu_g + (1 - \alpha_g) \mu_w] (\nabla \cdot \mathbf{v} + (\nabla \cdot \mathbf{v})^T) \end{aligned} \quad (2)$$

At this point, no assumption is needed for the constitutive equations of the turbulent stress  $\tau^T$ , the phase change volume generation  $\Gamma_g$ , the pressure distribution  $p_m$  and the mixture momentum source  $\mathbf{M}_m$ . These terms will be taken into account by means of macroscopic laws specifically derived for the 1D model.

2.2. One-dimensional homogeneous free-surface flow model

In many cases, the computational domain is essentially one-dimensional (cross-sectional velocities have no significant impact on the flow). The computation effort can be greatly reduced by simplifying two equations of momentum and area-integrating the remaining equations [13]. Such an area-integrated model gives full account of the flow in the predominating direction. Only friction correlations include the global effect of transversal mechanisms such that transversal velocities and accelerations are mostly neglected. This approach has been proven efficient in many cases. The originality of the present paper is to consider a free-surface flow in the integration process. It is indeed shown in the following how the free-surface set of equations can be used to simulate pressurized flow as well. It results in a 1D free-surface HE-Model (see Fig. 2).

For this purpose, a Cartesian coordinate system  $oxyz$  is set in such a way that  $x$ -axis is parallel to the predominating flow direction of the computational domain (Fig. 3). The whole process of integration is beyond the scope of this paper. The derivation is performed by analogy to the integration of the Saint-Venant equations for pure water flow as exposed in [13] but the basis equations are in this case a two-phase flow model. Briefly, momentum equations along both the  $y$ -axis and the  $z$ -axis are simplified by means of a non-dimensional analysis and reduce to a pressure distribution over the flow section:

$$\frac{\partial p_m}{\partial z} = -\rho_m g \sin \theta_z \quad \text{and} \quad \frac{\partial p_m}{\partial y} = 0 \quad (3)$$

where  $\theta_z$  is the slope between the  $z$ -axis and the global vertical.

Successive integrations over the flow width ( $y$ -abscissa) and the flow depth ( $z$ -abscissa) are performed on the basis of the Leibniz integral rule [13] and adapted boundary conditions at the bottom, free-surface and banks of the cross-section. The success of the method relies on choosing wisely the definition of the area-average. As a consequence, the area-average of a general function  $f$  is defined as:

$$\langle f \rangle(x, t) \triangleq \frac{1}{\Omega} \int_{\Omega} f(x, y, z, t) dA \quad (4)$$

where  $\Omega$  [ $m^2$ ] is the flow cross-section area. Likewise, the 1D mixture velocity is chosen as the mixture density weighted area-average of the 3D mixture velocity:

$$\tilde{u}_m \triangleq \frac{\langle \rho_m u_m \rangle}{\langle \rho_m \rangle} \quad (5)$$

The resulting field equations is written in terms of the conservative variables given by the following vector  $[(1 - \langle \alpha_g \rangle) \Omega; \langle \alpha_g \rangle \Omega; (1 - \langle \alpha_g \rangle) \tilde{u}_m \Omega]^T$ :

$$\begin{cases} \frac{\partial(1-\langle\alpha_g\rangle)\Omega}{\partial t} + \frac{\partial(1-\langle\alpha_g\rangle)\tilde{u}_m\Omega}{\partial x} = 0 \\ \frac{\partial\langle\alpha_g\rangle\Omega}{\partial t} + \frac{\partial\langle\alpha_g\rangle\tilde{u}_m\Omega}{\partial x} = \langle\Gamma_g\rangle\Omega \\ \frac{\partial(1-\langle\alpha_g\rangle)\tilde{u}_m\Omega}{\partial t} + \frac{\partial(1-\langle\alpha_g\rangle)\tilde{u}_m\tilde{u}_m\Omega}{\partial x} - g(1-\langle\alpha_g\rangle)\Omega\left(\frac{\partial Z}{\partial x} - S_F\right) + gp_w\frac{\partial\langle\alpha_g\rangle}{\partial x} = 0 \end{cases} \quad (6)$$

where the hydrostatic pressure  $p_w$  is given by:

$$p_w = \int_{-h_b}^{h_s} (h_s - z)l(z)dz \quad (7)$$

and  $Z$  [m] is the free surface elevation,  $S_F$  [-] is the friction slope (resulting from the integration of the viscous, turbulent shear stress and the interfacial momentum source). The free-surface height  $h_s$  is computed from the intersection between the  $x$ -axis and the cross-section. The distance between the bottom height and the intersection points is given by  $h_b$  (negative in the integration because the total height  $h = h_s - (-h_b)$ ). The local width is denoted  $l(z)$ .

To close the partial differential system, we still need to give an expression for the phase change volume generation  $\Gamma_g$ . Literature is abundant for empirical relations. To keep the generality of the model, a very fundamental relation given in [22] for air entrainment has been considered:

$$\langle \Gamma_g / \rho_g \rangle \Omega = -m\Gamma(\alpha_g - \alpha_{g,eq}) \quad (8)$$

where  $\Gamma$  and  $\alpha_{g,eq}$  are constants calibrated with experimental results (this last one is the equilibrium air concentration reached when the flow is fully developed). The onset of air entrainment is controlled by the parameter  $m = 1$  or  $m = 0$ .

2.3. Constitutive equation for the friction

Head loss in pressurized and free-surface single phase flow can be readily calculated by means of the Darcy–Weisbach equation [13] coupled with the Moody–Stanton diagram, the Blasius equation or the Colebrook implicit relation. However, additional head-loss has to be accounted for in two-phase flow. Due to the importance of a correct evaluation of the frictional pressure drop,

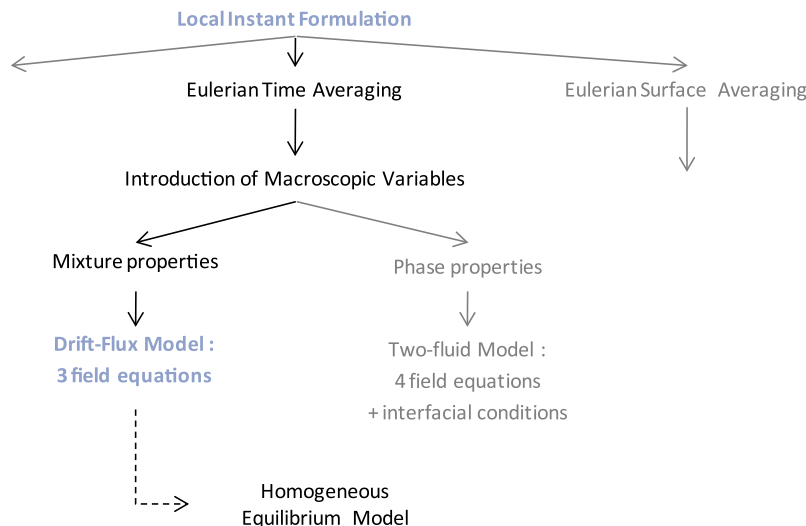


Fig. 2. Homogeneous equilibrium model is a time-integrated multiphase model.

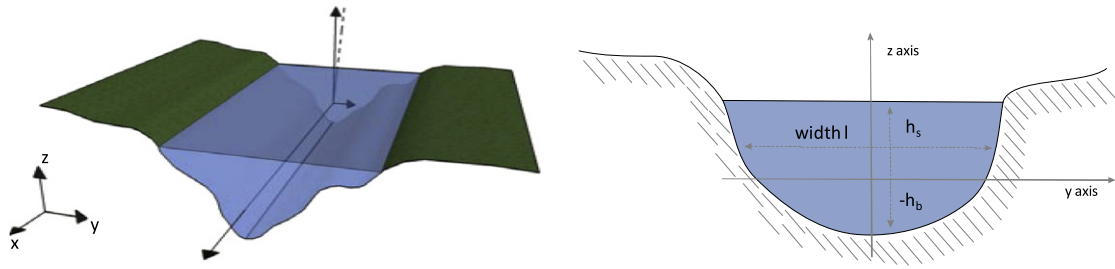


Fig. 3. Domain of integration includes a free surface.

the literature contains a plethora of engineering correlations for pipe friction, channel friction and some data for other interesting components such as pumps.

In this paper, a comparative study of the three most widespread correlations is performed from the point of view of civil and environmental engineering. In this respect, the homogeneous friction consists in using single-phase correlation with mixture parameters. On the opposite, the Lockhart–Martinelli correlation and the approach of Muller-Steinhagen and Heck are multiphase correlations that neglect the pipe roughness. The following section thus underlines a fundamental knowledge gap. On the one hand, single-phase correlations do not account for the phases interactions. On the other hand, multiphase correlations neglect pipe roughness. On large scale applications, both contributions are equally important and should be adequately accounted for.

### 2.3.1. Homogeneous friction

The hypothesis underlying this correlation is similar to the one made to develop the HE-Model. When the mixture is thoroughly mixed both air and water can be assumed to move at the same velocity and the frictional pressure drop can be approximated by the friction coefficient for a single phase flow calculated on the basis of suitable “mixture parameters”. This model is called homogeneous model [20,23] or no-slip model [24]. The most thorough discussion of the model is given by Wallis [20]. The frictional pressure gradient is then calculated by means of the Darcy–Weisbach equation:

$$-\left(\frac{dp}{dx}\right)_F = \langle \rho_m \rangle g \Omega S_F = \langle \rho_m \rangle f \frac{\tilde{u}_m^2}{2D_h} \Omega \quad (9)$$

where  $f$  is the friction factor and  $D_h$  is the hydraulic diameter.

In chemical and process engineering, the friction factor  $f$  is usually computed with an explicit Blasius-like correlation as follows:

$$f = \begin{cases} 64Re_f^{-1} & \text{if } Re_f \leq 2500 \\ 0.3164Re_f^{-0.25} & \text{if } Re_f > 2500 \end{cases} \quad (10)$$

In civil and environmental engineering, the implicit Colebrook–White correlation for the friction factor is generally preferred as it takes into account the pipe roughness as well:

$$f = \begin{cases} 64Re_f^{-1} & \text{if } Re_f \leq 2500 \\ \sqrt{f} = -2 \log \left( \frac{k_D}{3.7D_h} + \frac{2.51}{Re_f \sqrt{f}} \right) & \text{if } Re_f > 2500 \end{cases} \quad (11)$$

where  $k_D$  [m] is the roughness height. In both Eqs. (10) and (11), the Reynolds number  $Re$  is the mixture Reynolds defined as:

$$Re_{f,m} \triangleq \frac{\langle \rho_m \rangle \tilde{u}_m D_h}{\langle \mu_m \rangle} \quad (12)$$

The mixture viscosity  $\mu_m$  is approximated with rheological models that take into account the void fraction. Many correlations are available but the authors found that the McAdams formulation [25] gives the most reliable results:

$$\frac{1}{\langle \mu_m \rangle} = \frac{\langle x_g \rangle}{\mu_g} + \frac{1 - \langle x_g \rangle}{\mu_w} \quad \text{with} \quad \langle x_g \rangle = \frac{\langle \alpha_g \rangle \rho_{air}}{\langle \rho_m \rangle} \quad (13)$$

### 2.3.2. Lockhart–Martinelli correlation (LM)

Two-phase friction pressure drop are still nowadays commonly modeled on the basis of the classical theory established by Lockhart and Martinelli [26]. Two-phase flow is considered to be divided into liquid and gas streams. Correlations are constructed with the results for the frictional pressure gradient in single-phase pipe flows of each of the two fluids. They are calculated on the basis of the Darcy–Weisbach equation applied to each single-phase stream:

$$\begin{cases} -\left(\frac{dp}{dx}\right)_{F,w} = \rho_w f_{f,w} \frac{(\tilde{u}_m(1-\langle x_g \rangle))^2}{2D_h} \Omega & \text{for the water flow} \\ -\left(\frac{dp}{dx}\right)_{F,g} = \rho_g f_{f,g} \frac{(\tilde{u}_m \langle x_g \rangle)^2}{2D_h} \Omega & \text{for the air flow} \end{cases} \quad (14)$$

Friction factors are calculated by means of the modified Blasius-like Eq. (10). The best results are indeed obtained when setting  $f = 0.184Re_f^{-0.2}$  for turbulent flow.

The pressure drops computed this way are then correlated with the Lockhart–Martinelli parameter  $X^2$  which gives a measure of the degree to which the two-phase mixture behaves as the water rather than as the gas:

$$X^2 \triangleq \left(\frac{dp}{dx}\right)_{F,w} / \left(\frac{dp}{dx}\right)_{F,g} \quad (15)$$

In addition, the two-phase frictional pressure drop is expressed in terms of two-phase multipliers defined as:

$$\Phi_{f,w}^2 \triangleq \left(\frac{dp}{dx}\right)_F / \left(\frac{dp}{dx}\right)_{F,w} \quad \text{and} \quad \Phi_{f,g}^2 \triangleq \left(\frac{dp}{dx}\right)_F / \left(\frac{dp}{dx}\right)_{F,g} \quad (16)$$

In the initial paper of Martinelli and Lockhart [26], the relations of two-phase frictional pressure drops as a function of  $X^2$  was presented in graphical forms for the four flow regimes: turbulent–turbulent, viscous–turbulent, turbulent–viscous and viscous–viscous. For sake of easier numerical application, Chisholm [27] develop simplified equations:

$$\Phi_{f,w}^2 = 1 + \frac{N}{X} + \frac{1}{X^2} \quad \text{and} \quad \Phi_{f,g}^2 = 1 + N.X + X^2 \quad (17)$$

The coefficient  $N$  can thereby be set according to Table 1.

### 2.3.3. Approach of Muller-Steinhagen and Heck (MSM)

Müller-Steinhagen and Heck [28] suggested a new correlation for the prediction of the frictional pressure gradient in two-phase flow in pipes. The effort was explicitly aimed at developing an approach which is simpler in application but still reliable in terms of accuracy. According to them, the pressure drops of the respective single-phase flows are calculated as follows:

**Table 1**  
Coefficient  $N$  according to [27].

Liquid	Gas	$N$
Turbulent	Turbulent	20
Viscous	Turbulent	12
Turbulent	Laminar	10
Viscous	Laminar	5

$$\left(\frac{dp}{dx}\right)_{F,w0} = f_{f,w0} \frac{(\langle \rho_m \rangle \tilde{u}_m)^2}{2\rho_w D_h} = A_{MSH} \quad (18)$$

$$\left(\frac{dp}{dx}\right)_{F,g0} = f_{f,g0} \frac{(\langle \rho_m \rangle \tilde{u}_m)^2}{2\rho_g D_h} = B_{MSH} \quad (19)$$

The friction factors are computed with Blasius-like correlation (10) where the Reynolds numbers used are given by the two following relations

$$Re_{f,g0} = \frac{\langle \rho_m \rangle \tilde{u}_m D_h}{\mu_g} \quad \text{and} \quad Re_{f,w0} = \frac{\langle \rho_m \rangle \tilde{u}_m D_h}{\mu_w} \quad (20)$$

The equation developed for the roughly linear increase of the pressure drop with increasing quality for  $x < 0.7$  can be written:

$$G_{MSH} = A_{MSH} + 2(B_{MSH} - A_{MSH})\langle x_g \rangle \quad (21)$$

A superimposition of Eqs. (19) and (21) covers the full range of flow quality  $0 \leq \langle x_g \rangle \leq 1$ :

$$\left(\frac{dp}{dx}\right)_F = G_{MSH}(1 - \langle x_g \rangle)^{1/C} + B_{MSH}\langle x_g \rangle^C \quad (22)$$

A value of  $C = 3$  was found by curve fitting measured data.

To determine the reliability of the method, Müller-Steinhagen and Heck [28] assessed their correlation against a data bank containing 9313 measurements of pressure gradient for different fluids, different pipe diameter and different flow conditions. They reported accuracy similar to the more complicated methods. However, for engineering applications, Keller [29] shows this method does not reach the same degree of accuracy than the Lockhart–Martinelli correlation when compared to measurement on scale model.

2.3.4. Comparison of the methods

Since the presence of air alters not only friction correlations but also the kinetic term, correlations cannot be compared in all generality by means of a Moody-like diagram and a particularized case must be specified for the sake of comparison. We consider a pressurized flow in a circular pipe of 0.5 m of diameter. Fig. 4 gives the equivalent friction factor (defined as the pressure drop divided by the mixture kinetic energy) plotted

against the mixture Reynolds number (for a local void fraction of 10%) and against the local void fraction (for a discharge of 5 m<sup>3</sup>/s). Similar analyses have been made with various cross-section shapes, with various hydraulic diameters as well as in the case of free-surface flows. The following conclusions stay consistent. We conclude from Fig. 4 that homogeneous theory and MSM theory gives analogous results for smooth pipes and LM method gives slightly bigger friction factor, especially for laminar flow. However, if the pipe roughness becomes important, all the methods based on Blasius-like formulation underestimate the friction factor. Under the assumption that a small void fraction ( $\alpha_g < 5\%$ ) does not affect drastically the onset of a boundary layer at the pipe walls, homogeneous Colebrook–White correlation is consequently preferred since it takes into account the pipe roughness, which is a determinant parameter in civil and environmental engineering. On large scale applications, such approximation would become too important too be valid. Additional research is thus clearly required about multiphase friction correlation in civil engineering.

2.4. Extension to pressurized flow

Pressurized flows are commonly described through the Water Hammer equations [30] derived from the equations of continuity and motion in a closed pipe. According to the Preissmann slot model [8], pressurized flow can be equally calculated through the free-surface equations by adding a conceptual slot at the top of a closed pipe (Fig. 5b). When the water elevation is above the pipe crown, it provides a conceptual free-surface flow, of which the gravity wavespeed is given by  $c = \sqrt{g\Omega/T_s}$  ( $T_s$  is the slot width). Strictly speaking, the pressure wave celerity of a flow in a full pipe, referred by  $a$  [m/s], depends on the properties of the fluid, the pipe, and its means of support. In first approximation, its value is not dependant of the pressure value and may be computed on the basis of solid mechanics relations [30]. It is then easy to choose a slot width  $T_s$  which equalizes the gravity wavespeed  $c$  to the water hammer wavespeed  $a$ :

$$T_s \triangleq \frac{g\Omega}{a^2} \quad \text{with} \quad a^2 \triangleq \Omega \frac{dp}{d(\rho\Omega)} \quad (23)$$

Consequently, the slot width depends directly on the pipe section and the pressure wave celerity. In civil engineering, this section may range from 0.001 m<sup>2</sup> for the smaller pipes to 50m<sup>2</sup> for bigger pipes. In a similar manner, the pressure wave celerity may range from 100 m/s for very flexible pipes up to 1400 m/s for rigid pipe. The common equation to evaluate the celerity is given in [30]:

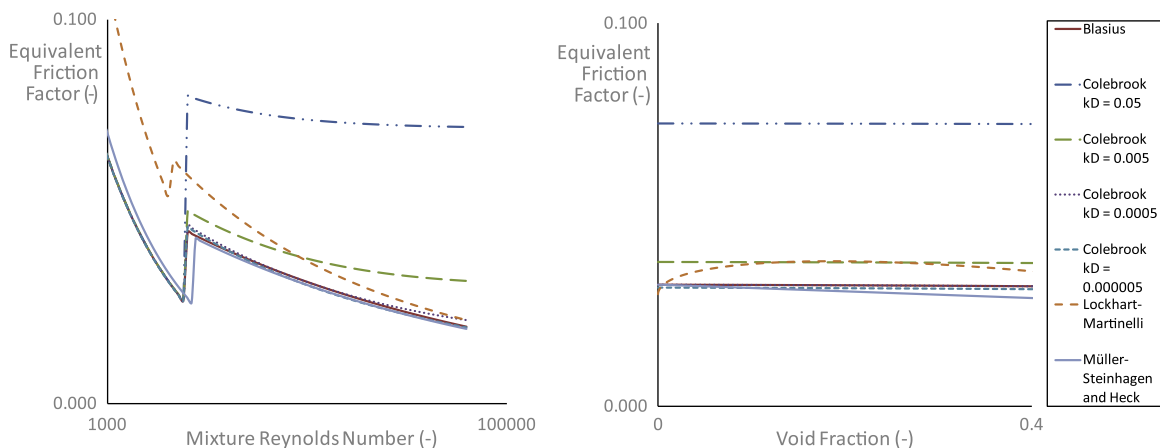


Fig. 4. Comparison between various friction correlations.

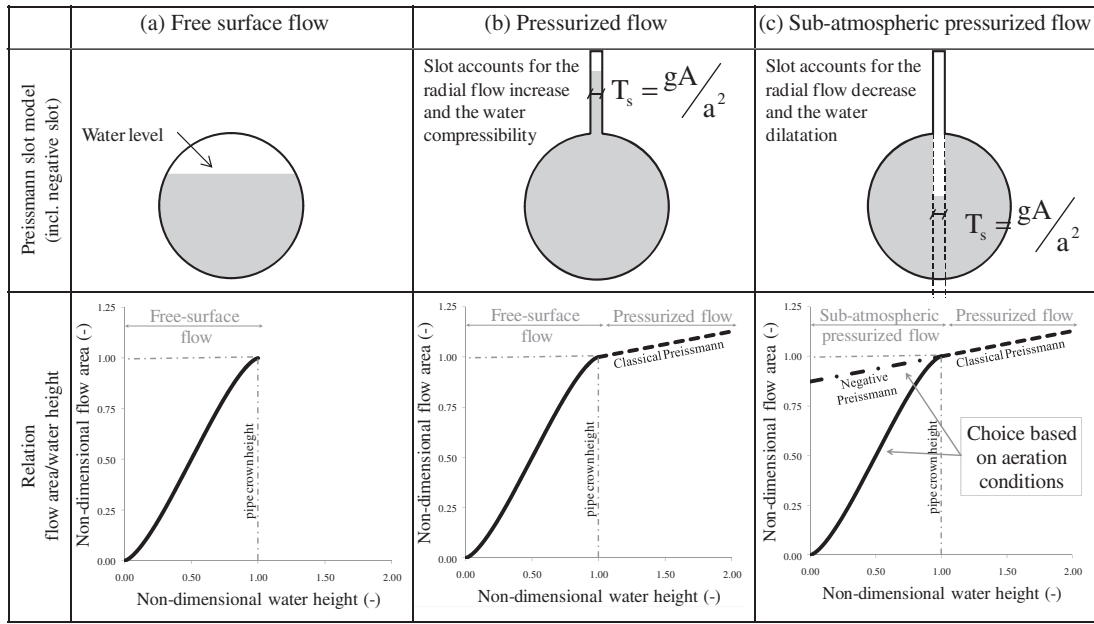


Fig. 5. The Preissmann slot method under different flow conditions.

$$a = \frac{\sqrt{K/\rho}}{\sqrt{1 + C^*K^*D/(E^*\Delta D)}} \quad (24)$$

where  $K$  and  $\rho$  are the bulk modulus of elasticity and density of the fluid,  $D$  and  $\Delta D$  are the inner diameter and the thickness of the pipe,  $E$  is the Young modulus (modulus of elasticity) of the pipe material, and  $C$  is a coefficient that accounts for the pipe support conditions.  $C = 1 - 0.5\mu$ , if pipe is anchored at the upstream end only.  $C = 1 - \mu/2$ , if pipe is anchored against any axial movement.  $C = 1$ , if each pipe section is anchored with expansion joints at each section.  $\mu$  represents the Poisson's ratio of the material. In presence of dispersed air, the celerity depends on the air concentration as well. According to Guinot [31], the celerity of a gas–liquid mixture is given by:

$$a_m = \frac{a}{\sqrt{1 + \langle \alpha_g \rangle \rho_{m,0} p_0^{1/\beta} / p^{1+\beta}}} \quad (25)$$

where the subscript 0 designates the reference state characterized by a pressure  $p = 101325$  Pa (atmospheric pressure).  $\beta$  is a coefficient equal to 1.0 for isothermal processes and 1.4 for adiabatic conditions. The reference void fraction  $\alpha_0$  is the volume fraction of dispersed air at reference pressure, and the  $\rho_{m,0}$  is the mixture density at reference pressure. As a consequence, the slot width may vary between  $5.10^{-9}$ m and  $5.10^{-2}$ m. However, the slot width must remain constant along the computation such that it does not take into account variation in air concentration. New methodologies are in development for enabling the slot to evolve along a computation [32].

From a hydraulic point of view, all the relevant information is summarized in the relation linking the water height and the flow area ( $H-\Omega$ ). A specific relation corresponds to each geometry of the cross section (Fig. 5a). Adding the Preissmann slot leads to linearly extend the relation beyond the pipe crown head.

The classical method of Preissmann assumes that the flow is correctly aerated everywhere. If the pressure drops below the atmospheric pressure, a free-surface appears above which the air is at atmospheric pressure. However, a lack of aeration devices in the pipe (like air vents, tanks, ...) prevent the apparition a free-surface. Any decrease in pressure below the atmospheric pressure causes the fluid dilatation and/or the pipe contraction. A sub-atmospheric pressurized flow appears. Classical Preissmann slot fails to

account for this kind of flows. In order to simulate such pressurized flows with a piezometric head below the pipe crown, the authors propose a new concept, called *negative Preissmann slot* [2].

As already said, any decrease in pressure below the atmospheric pressure causes the fluid dilatation and/or the pipe contraction. According to the linear theory of the mechanics of continuum means, the dilatation/contraction rate is exactly the same than for a pressurized flow. To put it in other words, the celerity of a pressurized flow remains constant even for sub-atmospheric pressure (and given by Eq. (24)). Because of this conclusion, extending the Preissmann straight line for water height below the pipe crown (Fig. 5c) in the relation linking the water height and the flow area ( $H-\Omega$ ) corresponds to a pressurized flow. The flow cross-section in this “negative slot” is smaller than the maximal section of the pipe (at atmospheric pressure). It explains the name negative Preissmann slot model. Physically, the storage capacity of the slot accounts for the fluid dilatation and/or the pipe contraction resulting from a decrease in pressure in the pipe.

As pointed in Fig. 5c, two values of the flow area corresponds to each water level below the pipe crown: one for the free surface flow and one for the pressurized flow. The choice between the two relations is done according to aeration conditions (closed pipe or presence of an air vent).

In transient flows, the slot width is imposed by the celerity through Eq. (23). Since we use an explicit numerical scheme, the time step  $\Delta t$  is limited by a CFL condition of the form:

$$NbC \leq 1 \quad \text{with } NbC \triangleq \max(|u_m| + c) * \frac{\Delta x}{\Delta t} \quad (26)$$

Practically, the velocity and the celerity are computed in each mesh and at each computational step. The maximum value of their addition limits the value of the time step. Usually, compute the time step by choosing a CFL Number  $NbC < 1$  that remain constant along the computation. The only way to increase the time step is thus to use coarser mesh. However, the wave celerity does not affect the steady state of a flow. Consequently, the choice of the slot width may be arbitrary for steady cases. Reducing the celerity augment the value of the time step one can use, without affecting the results. In this paper, we use a slot of 0.05 m.

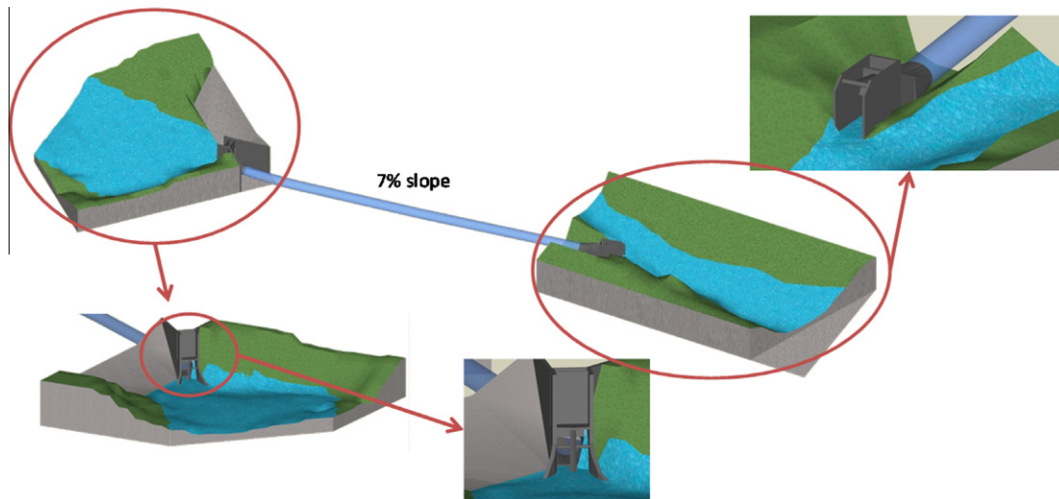


Fig. 6. Sketch of the experimental device.

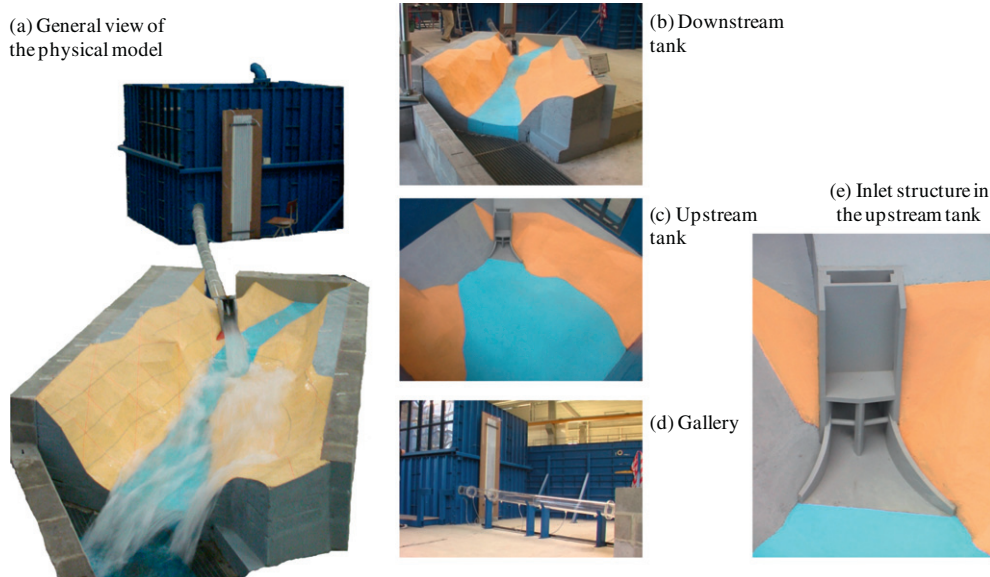


Fig. 7. Details of the physical model.

### 2.5. Numerical model

Discretization of Eq. (6) is performed by means of a finite volume scheme with an original flux vector splitting [33]. The scheme has been proven to be 1st order accurate and very robust. The time discretization is achieved with a classical 3-step Runge–Kutta algorithm [34]. Non linear stability analysis [35] shows that the Courant Number must be limited to 0.6 with this algorithm. The efficiency of such an explicit method is well known because of its low computation-cost. Moreover the coefficients have been tuned to emphasize the dissipation and the stability properties of the scheme. For steady flows, an improved formulation of the flux vector splitting enables to speed up the computation [36].

### 3. Application to aerated flows in gallery

In this section, numerical results are assessed by comparison with experimental results gained on a scale model (Fig. 6) build in the Laboratory of Engineering Hydraulics of the University of

Liege. The application considers only steady flows because guidelines consider only this kind of flows. Nevertheless, the approach has also been validated on transient benchmarks [9,37,38].

#### 3.1. Experimental set-up

The experimental facilities are made of two tanks, an upstream and a downstream one, linked by a 5 m long circular gallery with a 0.14 m diameter. The natural topography of a mountain river bed is represented in both tanks, as if the gallery bypassed a river meander. The gallery inlet and outlet are located in the right bank of the river, at the level of the river bottom. The constant gallery slope is 6.96%. The gallery inlet is designed to decrease head losses. A radial gate is placed at the outlet to control the discharge. The flow is there critical. The tanks are made of steel. The tanks topography has been build with concrete blocks and mortar painted with latex (Fig. 7). The gallery is in transparent Plexiglas and the inlet and outlet are made of aluminum and PVC. The roughness height of the gallery has been estimated to be  $2 \cdot 10^{-5}$  m. The water feeding

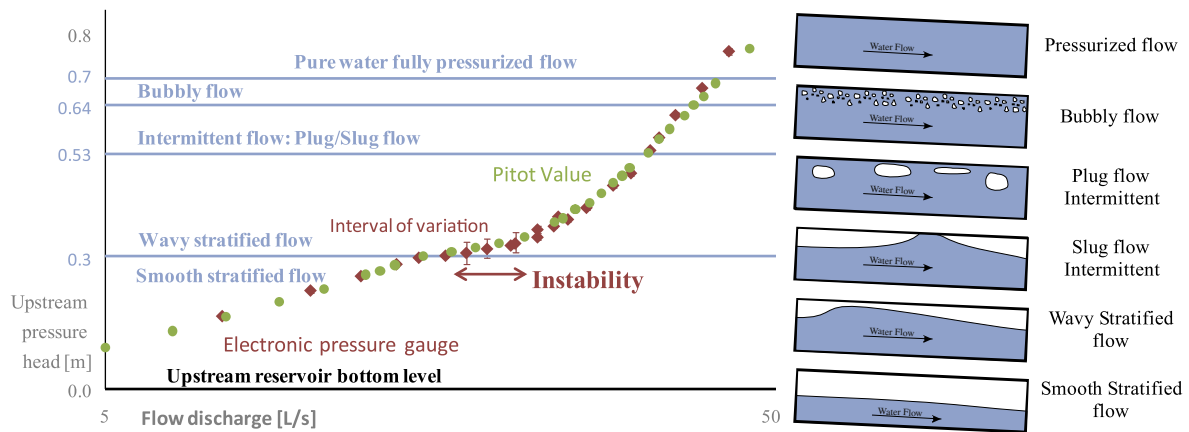


Fig. 8. Experimental discharge curve (upstream pressure head-flow discharge) and flow patterns.

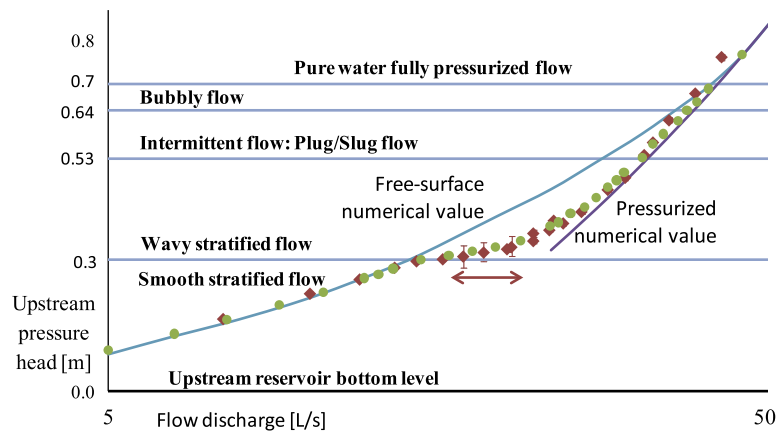


Fig. 9. Flow discharge relation for pure water simulations.

system is a closed circuit which injects water in the upstream tank and collects water flowing from the downstream tank. The discharge in the upstream tank is the upstream boundary condition. The head level upstream of the gallery regulates naturally regarding the gate opening rate and the system release capacity. Downstream of the physical model, the natural topography is very steep so no specific boundary condition is needed (trans-critical flow).

The model is equipped with the following measurement system. The upstream discharge is measured with an electromagnetic dischargemeter (accuracy of  $\pm 1$  L/s) on the pumping system. The water level in the upstream tank is measured using a limnimeter (accuracy of 0.1 mm), a Pitot tube (accuracy of  $\pm 0.1$  mm) and an electronic piezo-resistive transducer (accuracy of  $\pm 0.1$  mm, sampling rate of  $100 \text{ s}^{-1}$ ). Nine Pitot tubes and five electronic piezo-resistive transducers (accuracy of  $\pm 0.1$  mm, sampling rate of  $100 \text{ s}^{-1}$ ) are regularly distributed along the gallery to measure the pressure head in the gallery (accuracy of  $\pm 0.1$  mm). Fourteen graduated scales are fixed on the gallery perimeter to measure the water level for non-pressurized flows.

### 3.2. Results of the experimental investigations

Investigations consider only stationary flows which are observed to be strongly altered by air–water interaction. We aim at determining the flow discharge through the gallery as a function of the upstream pressure head. In particular, the flow discharge

through the gallery is strongly influenced by air/water interactions, and consequently depends of the aeration rate as well.

As pointed in Fig. 8, a flow discharge in the gallery is associated to a value of the upstream pressure head (zero level is set at the upstream reservoir bottom level) and to a specific two-phase flow pattern. The six flow patterns (Fig. 8) traditionally mentioned in the literature [20] are experienced in the gallery: smooth stratified flow, wavy stratified flow, intermittent flow that includes slug flow as well as plug flow, bubbly flow and pure water pressurized flow. What is more, a periodic instability originating from the variations in the aeration rate creates oscillation in the upstream tank. This instability was first evocated in [39] and is treated in details in [40].

### 3.3. Comparison with the results of the single phase model

In this section, simulations are performed under the assumption of a pure water flow (void fraction is equal to zero), with a spatial discretization step  $\Delta x = 3.33$  cm. Since a three step Runge–kutta scheme is used, the CFL number must be limited to 0.5 for stability reasons (this limitation results from non-linear stability analysis proposed in [35]). As exposed in section 0, the Homogenous Colebrook–White correlation is used with the McAdam formulation for the mixture viscosity and a roughness height  $k_D = 2.10^{-5}$  m. Comparison of results computed with other two-phase friction correlations is provided in section 0. The flow discharge varies between 5 L/s and 55 L/s. A first head/discharge relation (dotted line in Fig. 9) is computed with the HE-Model

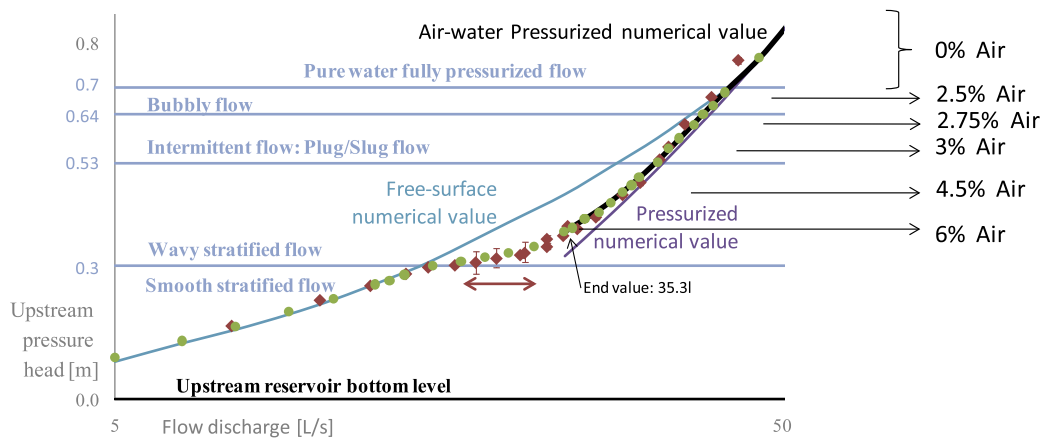


Fig. 10. Results in terms of upstream pressure head and concentration in the air–water mixture.

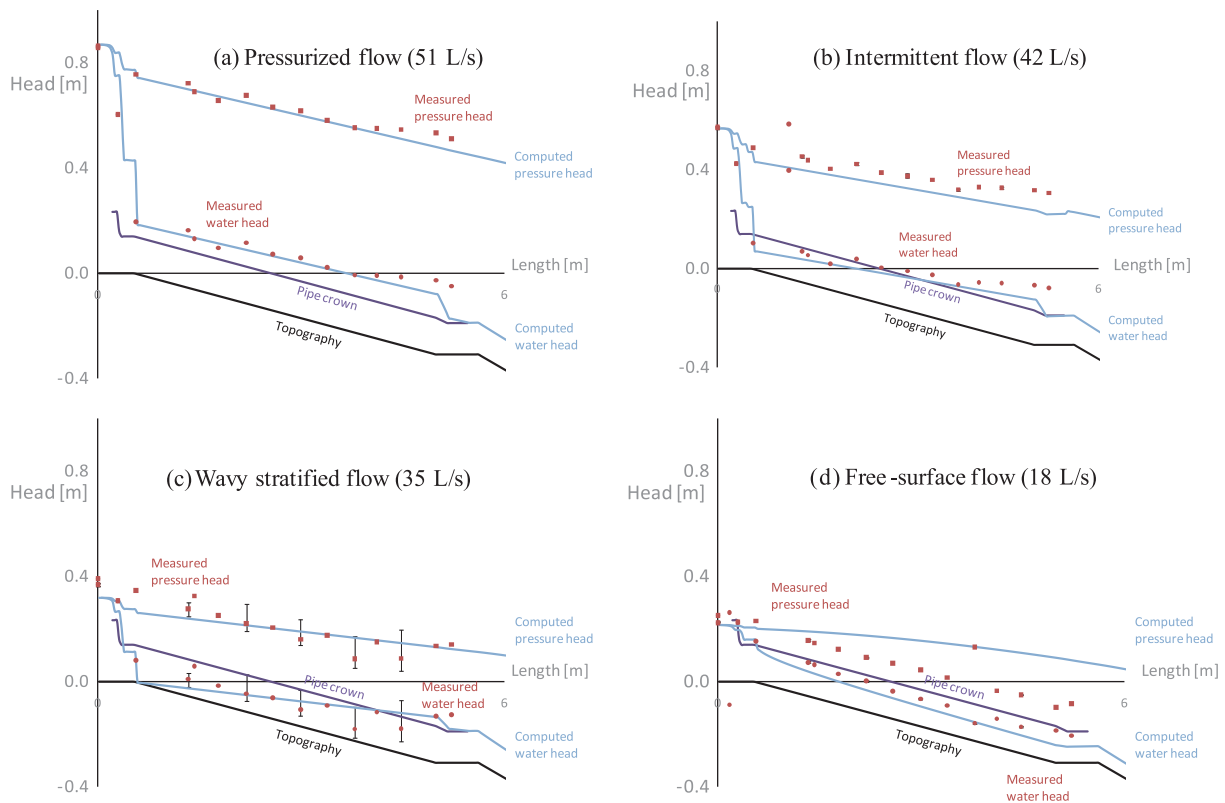


Fig. 11. Computed total head and pressure head distribution for a pressurized flow (51 L/s), for an intermittent flow (42 L/s), for a wavy stratified flow (35 L/s) and for a free-surface flow (18 L/s). The length along the pipe is measured from the entrance of the pipe inlet, while the level 0 of the head is the bottom of the inlet.

and assuming a free surface appears in each mesh if the water height is below the pipe crown (air phase above the free surface is at atmospheric pressure). The second head/discharge relation (continuous line) is computed by activating the negative Preissmann slot (sub-atmospheric pressurized flow). Numerical results are in good accordance with experimental data for smooth stratified flows and fully pressurized flows. Bubbly and intermittent flows show a similar behavior to the sub-atmospheric pressurized flows. The transition from pressurized to free-surface is subjected to a flow instability [39,40].

Experimental and numerical data for the distribution of the total head and the pressure head along the gallery length are given in Fig. 11 for a pressurized flow (51 L/s), for a wavy stratified flow (35 L/s) and for a free-surface flows (18 L/s). In the former case, re-

sults are in full agreement. For the intermittent flow, a slight discrepancy is observed in the total head curve. This discrepancy is exacerbated for wavy-stratified flows and free-surface flows. It results from the air–water interaction.

### 3.4. Comparison with results of the air–water homogeneous flow model

Application of the HE-Model enables to overcome the results discrepancy observed in the previous section by taking into account air–water interactions below the free-surface. The effect of the entrained air on the water flow is accurately computed by using the Eq. (8) for the phase change volume generation  $\Gamma_g$ . The parameter  $\Gamma$  is set at 25 and  $\alpha_g$  is calibrated according to the flow

**Table 2**  
Comparison of friction correlations.

	Upstream total head (cm)	Error (%)
Experimental	40.53	2.5
Homogeneous Colebrook	39.5036	2.5
Homogeneous Blasius	39.5027	2.5
Lockhart–Martinelli	39.5004	2.5
Müller–Steinhagen and Heck	39.5018	2.5

pattern observed (its value is given in Fig. 10). For bubbly flows, as bubbles arise from the air dissolved in water, equilibrium void fraction is chosen between 0.5% and 2%. For intermittent flows, an additional air supply is provided through a vertical vortex appearing at the water intake. Equilibrium void fraction is then chosen between 2% and 4.5%. Fig. 10 shows the discharge curve computed by assuming such a variation of the equilibrium void fraction.

### 3.5. Influence of the friction correlation

In this section, computation is performed for a bubbly flow of 36.5 L/s and a void fraction of 4.5%. The four friction correlations introduced above are considered: Homogeneous Colebrook–White ( $k_D = 2.10^{-5}$  m), Homogeneous Blasius, Lockhart–Martinelli and Müller–Steinhagen and Heck. Results in terms of the upstream total head, which is the parameter the most affected by the friction, are given in Table 2. Obviously, accuracy of the results is only slightly affected by the choice of the friction correlation. It results from the feeble roughness and air void fraction observed. However, simulation on large scale prototype exhibits important discrepancies. Further research is thus required to integrate both the effect of the pipe roughness and of the multiple phases.

## 4. Conclusion

In brief, the present paper exposed the derivation of the original mathematical model that we called one-dimensional free-surface homogeneous equilibrium and the numerical scheme used to solve it. Applicability of the model was extended to pressurized flow by using the Preissmann slot concept and introducing a negative Preissmann slot. Finally, numerical results are assessed by comparison with experimental results gained for steady flows on a scale model. In view of the rigorous theoretical background which underlies the derivation of the model as well as the good agreement obtained with experimental data, one might say the research gives new tools and results for developing a unified model for both free-surface and pressurized steady flows (mixed flow), for weak air/water interactions and which is suitable for multi-scale civil engineering applications. Findings accord with previous work and prove originality by area-integrating 3D HE-Model over a cross-section including a free-surface and simulating sub-atmospheric pressurized flow by means of the negative slot. What is more, our very general approach should remain valid for a wide range of environmental flows as sediment and pollutant transport phenomena. However, the model turns out to be limited in the sense he cannot describe accurately strong air–water interactions (counter-current air propagation as well as important pressure difference between phases are not mathematically modeled). What is more, it cannot describe essentially two- and three-dimensional flows as well rapidly moving transition (which requires a robust numerical scheme). Finally, further research is needed to handle relative velocities between the two phases (Drift-Flux model), to handle the air flowing above the free-surface (three-phase model) and en-

hance the robustness of the numerical scheme to simulate transient flows.

## References

- [1] Zhou F, Hicks FE, Steffler PM. Effects of trapped air during rapid filling of partially full pipes. In: Annual conference of the Canadian society for civil engineering; 2002.
- [2] Kerger F et al. Simulation numérique des écoulements mixtes hautement transitoire dans les conduites d'évacuation des eaux. *Houille Blanche-Rev Int* 2009;1(5):159–67.
- [3] Zhou F, Hicks FE, Steffler PM. Transient flow in a rapidly filling horizontal pipe containing trapped air. *J Hydraul Eng* 2002;128(6):625–34.
- [4] Guo Q, Song C. Dropshaft hydrodynamics under transient conditions. *J Hydraul Eng* 1991;117(8):1042–55.
- [5] Vasconcelos J, Wright S. Experimental investigation of surges in a stormwater storage tunnel. *J Hydraul Eng* 2005;131(10):853–61.
- [6] Cardle J, Song C. Measurement of mixed transient flows. *J Hydraul Eng* 1988;115(2):169–82.
- [7] Li J, McCorquodale A. Modeling mixed flow in storm sewers. *J Hydraul Eng* 1999;125(11):1170–80.
- [8] Preissmann A. Propagation des intumescences dans les canaux et rivières. In: First congress of the French association for computation. Grenoble, France; 1961.
- [9] Vasconcelos J, Wright S, Roe PL. Improved simulation of flow regime transition in sewers: the two-component pressure approach. *J Hydraul Eng* 2006;132(6):553–62.
- [10] Bourdarias C, Gerbi S. A finite volume scheme for a model coupling unsteady flows in open channels and in Pipelines. *J Comput Appl Math* 2007;209(1):109–31.
- [11] Bourdarias C, Gerbi S, Gisclon M. A kinetic formulation for a model coupling free surface and pressurized flows in closed pipes. *J Comput Appl Math* 2008;218(2):522.
- [12] Song C, Cardle J, Leung KS. Transient mixed-flow models for storm sewers. *J Hydraul Eng* 1983;109(11):1487–503.
- [13] Cunge JA, Holly FM, Verwey A. Practical aspects of computational river hydraulics. Monographs and surveys in water resources engineering. Boston: Pitman Advanced Pub. Program; 1980.
- [14] Politano M, Odgaard AJ, Klecan W. Numerical evaluation of hydraulic transients in a combined sewer overflow tunnel system. *J Hydraul Res* 2007;133(10):1103–10.
- [15] Vasconcelos JG, Wright SJ. Investigation of rapid filling of poorly ventilated stormwater storage tunnels. *J Hydraul Res* 2009;47(5):547–58.
- [16] Ishii M, Hibiki T. Thermo-fluid dynamics of two-phase flow. 1st ed. USA: Springer Science; 2006. p. 430.
- [17] Kerger F et al. Modelling flows in environmental and civil engineering. New-York: Nova Science Publishers; 2010. p. 155.
- [18] Hibiki T, Ishii M. One-dimensional drift-flux model for two-phase flow in a large diameter pipe. *Int J Heat Mass Transfer* 2003;46(10):1773–90.
- [19] Clerc S. Numerical simulation of the homogeneous equilibrium model for two-phase flows. *J Comput Phys* 2000;161:354–75.
- [20] Wallis GB. One-dimensional two-phase flow. 2nd ed. New York: McGraw-Hill; 1969. p. 410.
- [21] Guinot V. Godunov-type schemes: an introduction for engineers. Amsterdam: Elsevier Science BV; 2003. p. 480.
- [22] Dewals BJ, et al. Quasi 2D-numerical model of aerated flow over stepped chutes. In: 30th IAHR congress. Greece; 2003.
- [23] Brennen CE. Fundamentals of multiphase flows. Cambridge University Press; 2005.
- [24] Awad MM, Muzychka YS. Bounds on two-phase flow – part 1 – frictional pressure gradient in circular pipes. In: ASME international mechanical engineering congress and exposition. Orlando, Florida; 2005.
- [25] McAdams WH, Woods WK, Heroman LC. ASME Int Develop Heat Transf Part II. *Trans ASME* 1942;64(3):193–200.
- [26] Lockhart RW, Martinelli RC. Proposed correlation of data for isothermal two-phase, two-component flow in pipes. *Chem Eng Progress* 1949;45:39–48.
- [27] Chisholm D. Influence of pipe surface roughness on friction pressure gradient during two-phase flow. *J Mech Eng Sci* 1978;20(6):353–4.
- [28] Müller–Steinhagen H, Heck K. A simple friction pressure drop correlation for two-phase flow in pipes. *Chem Eng Process* 1986;20(6):297–308.
- [29] Keller U. Intermittent flow in hydraulic conduits. In: Versuchsanstalt für Wasserbau, Hydrologie und Glaziologie der Eidgenössischen. Zürich: ETH Zürich; 2006. p. 250.
- [30] Wylie EB, Streeter VL. Fluid transients. Première ed., M.-H. Inc; 1978. p. 385.
- [31] Guinot V. Numerical simulation of two-phase flow in pipes using Godunov method. *Int J Numer Methods Eng* 2001;50(5):1169–89.
- [32] Kerger F. Modelling transient air–water flows in civil and environmental engineering. In: ArGenCo. Liège: University of Liège; 2010. p. 310.
- [33] Dewals BJ et al. Depth-integrated flow modelling taking into account bottom curvature. *J Hydraul Res* 2006;44(6):787–95.
- [34] Leveque RJ. Finite volume methods for hyperbolic problems. Cambridge texts in applied mathematics. Cambridge University Press; 2002. p. 540.
- [35] Hirsch C. Numerical computation of internal and external flows – fundamentals of numerical discretization, vol. 1. Chichester: Wiley; 1988. p. 515.

- [36] Kerger F et al. A fast universal solver for 1d continuous and discontinuous steady flows in rivers and pipes. *Int J Numer Methods Fluids* 2011;66(1):38–48.
- [37] Leon A et al. Application of Godunov-type schemes to transient mixed flows. *J Hydraul Res* 2008;47(2).
- [38] Kerger F et al. An exact Riemann solver and a Godunov scheme for simulating highly transient mixed flows. *J Comput Appl Math* 2011;235(8):2030–40.
- [39] Mays L, editor. *Stormwater collection systems design handbook*. McGraw-Hill; 2001. p. 1008.
- [40] Erpicum S, et al. Experimental and numerical investigation of mixed flow in a Gallery. In: *Multiphase flow V*. New Forest: WIT Press; 2009.